

This document contains a post-print version of the paper

## A new flatness-based control of lateral vehicle dynamics

authored by **S. Antonov, A. Fehn, and A. Kugi**

and published in *Vehicle System Dynamics*.

---

The content of this post-print version is identical to the published paper but without the publisher's final layout or copy editing. Please, scroll down for the article.

---

### Cite this article as:

S. Antonov, A. Fehn, and A. Kugi, "A new flatness-based control of lateral vehicle dynamics", *Vehicle System Dynamics*, vol. 46, no. 9, pp. 789–801, 2008. DOI: [10.1080/00423110701602696](https://doi.org/10.1080/00423110701602696)

---

### BibTex entry:

```
@ARTICLE{acinpaper,  
  author = {Antonov, S. and Fehn, A. and Kugi, A.},  
  title = {A new flatness-based control of lateral vehicle dynamics},  
  journal = {Vehicle System Dynamics},  
  year = {2008},  
  volume = {46},  
  pages = {789--801},  
  number = {9},  
  doi = {10.1080/00423110701602696}  
}
```

---

### Link to original paper:

<http://dx.doi.org/10.1080/00423110701602696>

---

### Read more ACIN papers or get this document:

<http://www.acin.tuwien.ac.at/literature>

---

### Contact:

Automation and Control Institute (ACIN)  
Vienna University of Technology  
Gusshausstrasse 27-29/E376  
1040 Vienna, Austria

Internet: [www.acin.tuwien.ac.at](http://www.acin.tuwien.ac.at)  
E-mail: [office@acin.tuwien.ac.at](mailto:office@acin.tuwien.ac.at)  
Phone: +43 1 58801 37601  
Fax: +43 1 58801 37699

---

### Copyright notice:

This is an authors' accepted manuscript of the article S. Antonov, A. Fehn, and A. Kugi, "A new flatness-based control of lateral vehicle dynamics", *Vehicle System Dynamics*, vol. 46, no. 9, pp. 789–801, 2008. doi: [10.1080/00423110701602696](https://doi.org/10.1080/00423110701602696) published in *Vehicle System Dynamics*, copyright © Taylor & Francis Group, LLC, available online at: <http://dx.doi.org/10.1080/00423110701602696>

## A New Flatness Based Control of Lateral Vehicle Dynamics

SERGIY ANTONOV\*†, ACHIM FEHN†, ANDREAS KUGI ‡

†Dept. CC/ESM1, Chassis Systems Control, Robert Bosch GmbH, P.O. Box 1355, 74003 Heilbronn, Germany

‡Automation and Control Institute, Complex Dynamical Systems Group, Vienna University of Technology,  
1040 Vienna, Austria

(v1.1 released June 2007, first submission January 2006)

This paper presents a new concept for Vehicle Dynamics Control (VDC). The control of the longitudinal vehicle dynamics is not discussed, since we are assuming that it is much slower and weakly coupled to the lateral and yawing dynamics. The actuators are considered to be the traction and the braking torques of the individual wheels and only the standard sensors of the common VDC system are used. A modular interface to the subordinate wheel control system is provided by choosing the yaw torque as a fictitious control input. The VDC system is designed by means of a two degrees-of-freedom control scheme. It is comprised of a flatness based feedforward part and a stabilizing feedback part. The reference trajectory generation is introduced for the flat output which is given by the lateral velocity of the vehicle. In this way an advantageous kind of body side-slip angle control is provided by means of standard VDC system hardware. Extensive simulation studies show the excellent performance of the designed control concept.

*Keywords:* vehicle dynamics control, differential flatness, two degrees-of-freedom control, trajectory generation

### 1 Introduction

This paper deals with the Vehicle Dynamics Control (VDC) design for passenger vehicles. The first series production VDC system was introduced by Robert Bosch GmbH [1] in 1994. The main purpose of this VDC system is to support the driver in critical driving situations by ensuring better controllability of the vehicle. This task is achieved by maintaining an almost identical vehicle behavior in all driving situations [2]. For this purpose the lateral dynamics of the vehicle are controlled. In this VDC system the braking and the traction torques of the individual wheels serve as the control inputs. Over the years VDC has shown great performance in accident prevention [3,4]. The effectiveness and the reduction in the production costs have facilitated the propagation of VDC as a standard equipment in many passenger vehicles.

Many reports dealing with VDC were published in recent years, e.g. [1, 5–8]. Different authors have treated the vehicle dynamics control task as a nonlinear optimization problem and developed different solutions [9–11]. In [9] the side-slip angle of the vehicle is limited by using the receding horizon approach and by minimizing the tire slips. The optimal solution is approximated by means of multiparametric nonlinear programming. The contribution [10] solves a convex optimization problem to keep all tires as far below their adhesion limits as possible. In [11] the authors aim at minimizing the tire slips and then present control laws based on a nonlinear optimization technique in combination with singular perturbation theory. Another trend in the literature is the use of differential geometric methods for the control design. Solutions by means of exact input-output linearization are proposed in [12, 13]. The differential flatness technique is adopted for vehicle dynamics control in the contributions [14, 15]. Therein the centralized longitudinal tire forces and the steer angle of the front wheels are chosen as control inputs. The corresponding flat output is identified as the longitudinal and lateral velocity components of a certain point located on the vehicle's longitudinal axis. This approach, although very interesting, suffers from the facts that the flat

\*Corresponding author. e-mail: sergiy.antonov@de.bosch.com

output depends on the vehicle mass and the moment of inertia about the vertical axis and that the control law relies on quantities which are not directly available by measurements in a common VDC system. In general, the common problem of the differential geometric and flatness based approaches is the generation of reasonable and sufficiently differentiable reference trajectories. In recent publications [12–15] this question is not explicitly treated.

Therefore, the focus of this paper is to close the gap between the reference trajectory generation and the design of a complete flatness based VDC system which is based on the standard interface for the actuator inputs and sensor information of common passenger vehicles. For this purpose the longitudinal vehicle dynamics is assumed to be much slower and weakly coupled with the lateral and yawing dynamics. This is why we will consider the longitudinal vehicle velocity as a known constant exogenous input of the VDC system. The longitudinal dynamics control systems available in the vehicle, like the Antilock Braking System (ABS) and the Traction Control System (TCS), are using individual wheel torques as control inputs. To allow for a modular system design, as it is usually done in the existing vehicle control concepts, the yaw torque is chosen as a suitable control input. It is used as a common interface in the vehicle dynamics control design, see for example [1, 6]. The corresponding wheel torque distribution can be calculated by the given acceleration or deceleration demand with regard to the requested yaw torque. Note that the maximum transmittable yawing torque depends on the actual grip conditions and results from the tires' saturation margin. The input of the VDC system, i.e. the driver's command, is specified through the measured steering angle and the actual longitudinal vehicle velocity. The control is based on the two degrees-of-freedom tracking control structure described in [16, 17]. It consists of the reference generation, the feedforward control by means of an inverse system description and the stabilizing feedback. In our case the reference generation relies on the linear vehicle model. In contrast to the known approaches [1, 7] the lateral vehicle velocity is chosen as the reference variable and not the yaw rate. In this way we are achieving more agile vehicle response to the driver's input. Another feature is that the knowledge of the actual grip conditions is not necessary for the reference calculation. The proposed feedforward control utilizes the flatness property of the nonlinear single-track vehicle model. The time derivative of the lateral velocity is used as a feedback variable to stabilize the system. Thus, the presented approach only relies on the standard VDC equipment of common vehicles, i.e. additional sensors or actuators are not required.

The paper is organized as follows. In Section 2 a nonlinear single-track vehicle model is presented. It builds the basis for the subsequent nonlinear control design. Afterwards the linear vehicle model is introduced for the purpose of reference trajectory generation. In Section 3 the differential flatness property of the nonlinear vehicle model is proven. Section 4 deals with the vehicle dynamics control design. In Section 5 the stability issues are discussed. The performance and the robustness of the developed concept are shown in Section 6 by means of simulations with a detailed multibody vehicle model. Finally, in Section 7 the results are summarized and an outlook is given.

## 2 Mathematical vehicle modeling

In this section two vehicle models are introduced: the first model provides the basis for the model based control design, and the second model is suited for the reference generation.

### 2.1 Vehicle model for control design

The vehicle model for control design is based on the single-track model which goes back to the work [18]. As proposed in [18] the two wheels of one axle are merged to one wheel (see Figure 1). Therefore, this model is also well known as the bicycle model [19, 20]. The following assumptions are made:

- the vehicle is a rigid body and has only front steering;
- there is neither roll nor pitch motion;
- the vehicle center of mass lies in the road plane, i.e. there is no dynamic wheel load distribution;
- the wheel dynamics are of minor importance;
- the longitudinal dynamics of the vehicle are not considered;

- the air drag is neglected.

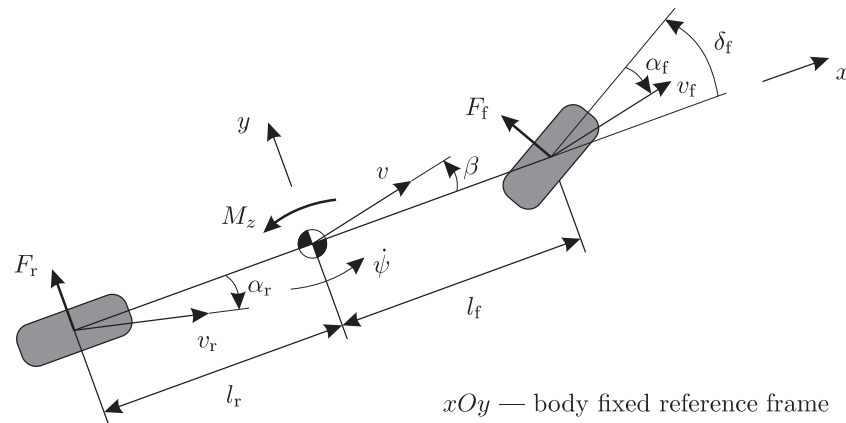


Figure 1. Nonlinear single-track vehicle model.

The considered vehicle (see Figure 1) has the mass  $m$  and the moment of inertia about the vertical axis  $I_z$ . The distances from the center of mass to the front axle and to the rear axle are given by  $l_f$  and  $l_r$ , respectively. The steer angle of the front wheel is given by  $\delta_f$  and the side-slip angle of the vehicle is denoted by  $\beta$ . The velocities of the front  $v_f$  and the rear axle  $v_r$  differ from the velocity of the center of gravity  $v$  due to the yawing motion  $\dot{\psi}$ . The velocity  $v$  has the longitudinal  $v_x$  and the lateral  $v_y$  projections on the body fixed reference frame  $xOy$ . The forces acting on the contact patch of the tires are centralized for each axle. They are known as effective axle forces  $F_f$  and  $F_r$  and result from the side-slip angles at the front and the rear axle,  $\alpha_f$  and  $\alpha_r$ , respectively. As previously mentioned the yaw torque  $M_z$  is introduced as a fictitious control input. The longitudinal vehicle velocity  $v_x$  is assumed to be a known constant  $v_x = \text{const}$ .

The effective axle forces  $F_f$  and  $F_r$  are functions of the corresponding side-slip angles  $\alpha_f$  and  $\alpha_r$  [20], i.e.

$$F_f = F_f(\alpha_f) \quad \text{and} \quad F_r = F_r(\alpha_r). \quad (1)$$

Typical characteristics of the effective axle forces  $F(\alpha)$  for passenger vehicles are depicted in Figure 2. These functions represent the main nonlinearities in the considered vehicle model. Normal drivers are using the vehicle with lateral accelerations of less than  $5 \text{ m/s}^2$  [21], which corresponds to the approximately linear region of the effective axle force characteristics, cf. Figure 2. However, if the vehicle moves on the road with reduced grip conditions, i.e. on a wet or icy road, then the axle force characteristics change according to the dotted line in Figure 2. In this case the nonlinear part of the force characteristics also applies for small lateral accelerations.

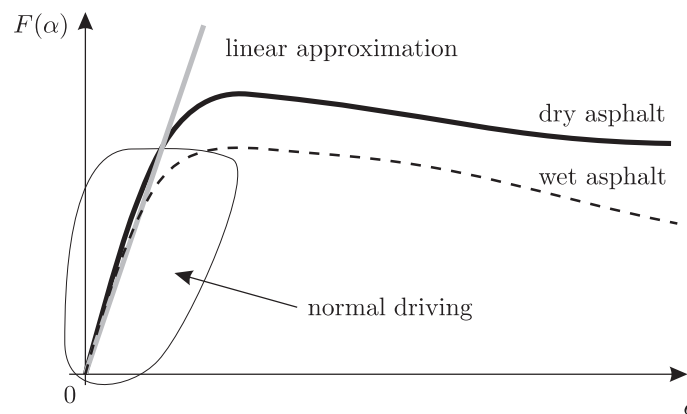


Figure 2. Typical characteristics of the effective axle forces for passenger vehicles, black solid line corresponds to dry asphalt, dotted line to wet asphalt, and grey solid line shows the linear approximation for normal driving situations.

Since the vehicle is considered as a rigid body the side-slip angles of the front and rear axle,  $\alpha_f$  and  $\alpha_r$ , and the body side-slip angle  $\beta$  take the form [19]

$$\alpha_f = -\arctan\left(\frac{v_y + \dot{\psi}l_f}{v_x}\right) + \delta_f \quad , \quad \alpha_r = -\arctan\left(\frac{v_y - \dot{\psi}l_r}{v_x}\right) \quad \text{and} \quad \beta = \arctan\left(\frac{v_y}{v_x}\right) . \quad (2)$$

The equations of motion for the vehicle's center of mass are given by

$$\frac{d}{dt}v_y = \frac{1}{m}\left(F_f(\alpha_f)\cos\delta_f + F_r(\alpha_r)\right) - v_x\dot{\psi} , \quad (3a)$$

$$\frac{d}{dt}\dot{\psi} = \frac{1}{I_z}\left(F_f(\alpha_f)l_f\cos\delta_f - F_r(\alpha_r)l_r + M_z\right) . \quad (3b)$$

The lateral acceleration of the vehicle is calculated by

$$a_y = \frac{d}{dt}v_y + v_x\dot{\psi} . \quad (4)$$

## 2.2 Reference vehicle model

As already mentioned in the previous subsection the field of experience of a normal driver lies in the linear region of the effective axle force characteristics, cf. Figure 2. Thus, the expected vehicle behavior can be described by assuming linear effective axle force characteristics, see for example the solid grey line in Figure 2. In this case the effective axle forces are given by

$$F_f(\alpha_f) = c_f\alpha_f \quad \text{and} \quad F_r(\alpha_r) = c_r\alpha_r , \quad (5)$$

where  $c_f$  and  $c_r$  are the so-called cornering stiffnesses of the front and rear axles, respectively. Substituting (5) into (3) and considering a small angle approximation in (2), i.e.  $\arctan\left(\frac{v_y + \dot{\psi}l_f}{v_x}\right) \approx \frac{v_y + \dot{\psi}l_f}{v_x}$  and  $\arctan\left(\frac{v_y - \dot{\psi}l_r}{v_x}\right) \approx \frac{v_y - \dot{\psi}l_r}{v_x}$  as well as  $\cos\delta_f \approx 1$ , we get the linear single-track vehicle model in the form

$$\frac{d}{dt}\begin{bmatrix} v_y \\ \dot{\psi} \end{bmatrix} = \begin{bmatrix} -\frac{c_r + c_f}{mv_x} & \frac{c_rl_r - c_fl_f}{mv_x} - v_x \\ \frac{c_rl_r - c_fl_f}{I_zv_x} & -\frac{c_rl_r^2 + c_fl_f^2}{I_zv_x} \end{bmatrix} \begin{bmatrix} v_y \\ \dot{\psi} \end{bmatrix} + \begin{bmatrix} \frac{c_f}{m} \\ \frac{c_fl_f}{I_z} \end{bmatrix} \delta_f + \begin{bmatrix} 0 \\ \frac{1}{I_z} \end{bmatrix} M_z . \quad (6)$$

In the following the external yaw torque  $M_z$  is considered to be zero, since the reference model must describe the vehicle behavior without VDC interventions. Then, for a constant steer angle  $\delta_{f0}$ , an equilibrium point  $(v_{y0}, \dot{\psi}_0)$  of the system (6) is given by

$$v_{y0} = -\frac{mv_x^3c_fl_f - v_xc_fc_r(l_r^2 + l_fl_r)}{mv_x^2(c_rl_r - c_fl_f) + c_fc_r(l_f + l_r)^2}\delta_{f0} = k_v(v_x)\delta_{f0} , \quad (7a)$$

$$\dot{\psi}_0 = \frac{v_xc_fc_r(l_f + l_r)}{mv_x^2(c_rl_r - c_fl_f) + c_fc_r(l_f + l_r)^2}\delta_{f0} = k_\psi(v_x)\delta_{f0} . \quad (7b)$$

It can be easily shown by means of the Routh-Hurwitz stability criterion that the equilibrium point (7) is asymptotically stable iff the following condition holds [19]:

$$mv_x^2(c_rl_r - c_fl_f) + c_fc_r(l_f + l_r)^2 > 0 . \quad (8)$$

Equations (7) represent the static linear vehicle model. Thus, they can be used to describe the quasi-static vehicle response on the steer input  $\delta_f$ . Consequently, they serve as a suitable reference model to specify agile vehicle behavior. Please note that equation (7b) is the well known Ackermann's equation [19].

### 3 Flatness property of the vehicle model

In the last years the *differential flatness* technique [17, 22–25] has gained popularity for the purpose of nonlinear tracking control design. In this section the differential flatness property of the dynamical system (3) is shown for the flat output  $y = v_y$  by calculating the corresponding inverse system. The steer angle  $\delta_f$  and the longitudinal vehicle velocity  $v_x = \text{const.}$  represent the driver's command. Thus, the steer angle  $\delta_f$  is considered as a sufficiently smooth known time function  $\delta_f = \delta_f(t)$ . It can be calculated from the measured steering wheel angle  $\delta_{\text{hand}}(t)$  by means of the corresponding kinematic transformation.

In a first step we will express the yaw rate  $\dot{\psi}$  as a function of the flat output  $y = v_y$ , its time derivative  $\dot{y} = \dot{v}_y$  and the exogenous input  $\delta_f(t)$  by utilizing (3a) with (2)

$$m\dot{y} - F_f \left( \delta_f - \arctan \left( \frac{y + \dot{\psi}l_f}{v_x} \right) \right) \cos(\delta_f) - F_r \left( -\arctan \left( \frac{y - \dot{\psi}l_r}{v_x} \right) \right) + mv_x\dot{\psi} = 0. \quad (9)$$

Clearly in view of Figure 2, equation (9) constitutes an implicit relation which cannot be solved analytically in the general case. In the linear region of the axle force characteristics for small angles, i.e.  $F_f(\alpha_f) = c_f(\delta_f - \frac{y + \dot{\psi}l_f}{v_x})$ ,  $F_r(\alpha_r) = c_r(-\frac{y - \dot{\psi}l_r}{v_x})$  and  $\cos(\delta_f) = 1$ , the parametrization of the yaw rate  $\dot{\psi}$  according to equation (9) is unique and reads as

$$\dot{\psi} = \frac{v_x c_f \delta_f - (c_f + c_r)y - v_x m \dot{y}}{c_f l_f - c_r l_r + mv_x^2}. \quad (10)$$

Due to the fact that the axle force characteristics  $F_f(\alpha_f)$  and  $F_r(\alpha_r)$  are not monotonously increasing, cf. Figure 2, the solution of the implicit equation (9) is no longer unique outside the linear region. However, since the steer angle  $\delta_f$ , as well as the flat output  $y$  and its time derivative  $\dot{y}$  are continuous, the solution of equation (9) for the yaw rate  $\dot{\psi}$  must be continuous as well. Thus, in the case of multiple solutions we choose  $\dot{\psi}$  which is closest to the one determined in the previous time step. Please note that we are always starting in the linear region, where the solution of (9) is equal to the solution of (10). This approach allows us to resolve the uniqueness problem and provides the physically relevant solution  $\dot{\psi} = \rho_1(y, \dot{y}, \delta_f)$ . Differentiating (9) w.r.t. time  $t$ , we get

$$m\ddot{y} - \frac{\partial}{\partial \alpha_f} F_f(\alpha_f) \left( \dot{\delta}_f - \frac{v_x(\dot{y} + \ddot{\psi}l_f)}{v_x^2 + (y + \dot{\psi}l_f)^2} \right) \cos(\delta_f) + F_f(\alpha_f) \sin(\delta_f) \dot{\delta}_f + \frac{\partial}{\partial \alpha_r} F_r(\alpha_r) \left( \frac{v_x(\dot{y} - \ddot{\psi}l_r)}{v_x^2 + (y - \dot{\psi}l_r)^2} \right) + v_x \ddot{\psi} = 0. \quad (11)$$

Thus the parametrization  $\ddot{\psi} = \rho_2(y, \dot{y}, \ddot{y}, \delta_f, \dot{\delta}_f)$  yields

$$\ddot{\psi} = \frac{\frac{\partial}{\partial \alpha_f} F_f(\alpha_f) \dot{\delta}_f \cos(\delta_f) - \frac{\partial}{\partial \alpha_f} F_f(\alpha_f) \frac{v_x \dot{y}}{v_x^2 + (y + \dot{\psi}l_f)^2} \cos(\delta_f) - \frac{\partial}{\partial \alpha_r} F_r(\alpha_r) \frac{v_x \dot{y}}{v_x^2 + (y - \dot{\psi}l_r)^2} - m\ddot{y} - F_f(\alpha_f) \sin(\delta_f) \dot{\delta}_f}{mv_x + \frac{\partial}{\partial \alpha_f} F_f(\alpha_f) \frac{l_f v_x}{v_x^2 + (y + \dot{\psi}l_f)^2} \cos(\delta_f) - \frac{\partial}{\partial \alpha_r} F_r(\alpha_r) \frac{l_r v_x}{v_x^2 + (y - \dot{\psi}l_r)^2}}, \quad (12)$$

with  $\alpha_f$  and  $\alpha_r$  from (2) and  $\dot{\psi} = \rho_1(y, \dot{y}, \delta_f)$  due to (9). Note that the axle characteristics  $F_f(\alpha_f)$  and  $F_r(\alpha_r)$

should be chosen for the controller design in order to guarantee that the denominator in (12) is not equal to zero, which is normally the case for higher longitudinal velocities  $v_x$ . By substituting  $\ddot{\psi} = \rho_2 (y, \dot{y}, \ddot{y}, \delta_f, \dot{\delta}_f)$  from (12) and  $\dot{\psi} = \rho_1 (y, \dot{y}, \delta_f)$  due to (9) into (3b), we directly obtain the parametrization of the control input, i.e. the yaw torque  $M_z$ , in the form

$$M_z = \rho_3 (y, \dot{y}, \ddot{y}, \delta_f, \dot{\delta}_f) = I_z \rho_2 (y, \dot{y}, \ddot{y}, \delta_f, \dot{\delta}_f) - F_f (\alpha_f) l_f \cos (\delta_f) - F_r (\alpha_r) l_r . \quad (13)$$

In summary, we have shown that the lateral velocity  $v_y$  serves as a flat output for the nonlinear single track model (2), (3).

#### 4 Control approach

In this section the flatness based VDC scheme is introduced. We are suggesting to use the two degrees-of-freedom control scheme as discussed in [16, 17]. Thereby, the trajectory tracking problem is tackled by means of a flatness based feedforward and a stabilizing feedback part in the controller. The trajectory planning is carried out in the coordinates of the flat output. The corresponding block diagram is depicted in Figure 3.

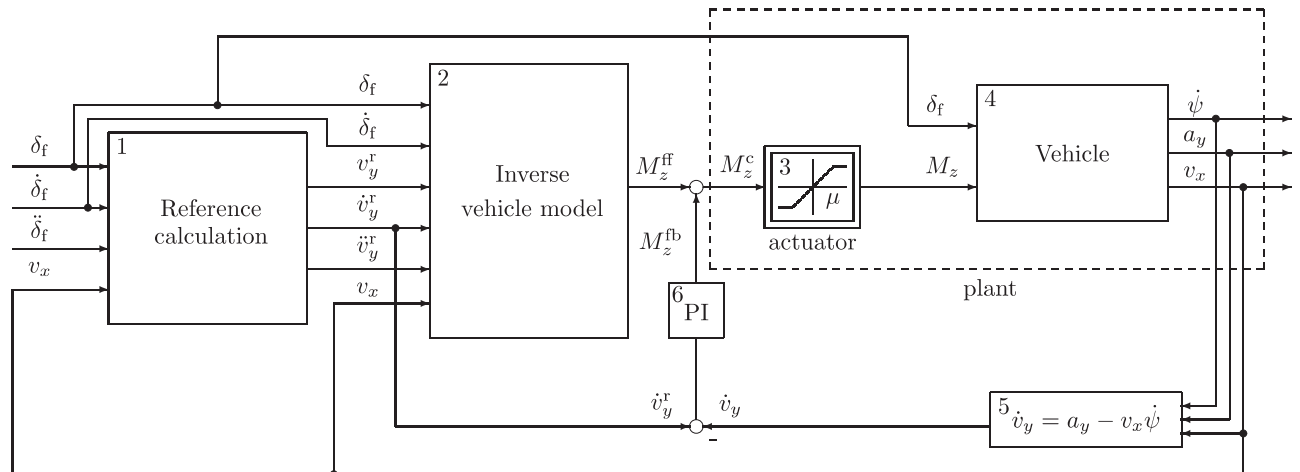


Figure 3. Block diagram of the vehicle dynamics control.

The reference trajectory  $v_y^r$  for the flat output is calculated in *Block 1* of Figure 3. As an appropriate reference model the static linear vehicle model (7) is chosen to provide the maximum possible agility of the closed-loop system and a driving feeling like in normal driving situations. Please note that equation (7b) is the well known Ackermann's equation which is traditionally used in the series-production VDC for the reference values generation [1]. In contrast to this we are proposing to use (7a) and its time derivatives up to the second order for the reference calculation<sup>1</sup>:

$$v_y^r = k_v(v_x) \delta_f , \quad \dot{v}_y^r = k_v(v_x) \dot{\delta}_f \quad \text{and} \quad \ddot{v}_y^r = k_v(v_x) \ddot{\delta}_f . \quad (14)$$

This approach is motivated by the fact that the lateral velocity  $v_y$  is directly related to the side-slip angle of the vehicle  $\beta$  via (2). In the case of small body side-slip angle  $\beta$  and constant longitudinal vehicle velocity  $v_x$  the lateral velocity is even proportional to the side-slip angle, i.e.  $\beta \approx v_y/v_x$ . By controlling

<sup>1</sup>Note that the reference model requires the knowledge of the steer angle  $\delta_f$  and its time derivatives up to the second order  $\dot{\delta}_f, \ddot{\delta}_f$ . The steer angle of the front wheel  $\delta_f$  can be simply calculated out of the measured steering wheel angle  $\delta_{hand}$ . The required time derivatives  $\dot{\delta}_f$  and  $\ddot{\delta}_f$  can be obtained for example by means of the *derivative estimator* proposed e.g. in [26].

the lateral velocity  $v_y$  of the vehicle, we indirectly control the side-slip angle and thus directly address the driving feeling and the vehicle stability. Furthermore, we avoid the consideration of the actual grip conditions. In contrast, classical VDC approaches are based on a yaw rate control concept. Therefore, in order to limit the side-slip angle, a bound on the reference yaw rate  $\dot{\psi}^r$  depending on the actual grip conditions has to be imposed. The valuable feature of our approach is the changeover to the control of the lateral velocity  $v_y$ .

The inverse system description (*Block 2*) is used as a feedforward part. It is based on (13) and yields the feedforward yaw torque  $M_z^{\text{ff}}$

$$M_z^{\text{ff}} = \rho_3(v_y^r, \dot{v}_y^r, \ddot{v}_y^r, \delta_f, \dot{\delta}_f) . \quad (15)$$

The input of the feedforward control is the driver's command in the form of the steering motion  $\delta_f, \dot{\delta}_f$  and the actual vehicle velocity  $v_x$ . Additionally, the reference values for the lateral vehicle velocity  $v_y^r$  and its time derivatives up to the second order,  $\dot{v}_y^r$  and  $\ddot{v}_y^r$ , are provided according to (14). The robustness of the considered control scheme as to disturbances and parameter variations is assured by means of the stabilizing feedback of the time derivative of the lateral velocity  $\dot{v}_y$  (*Block 5*)

$$\dot{v}_y = a_y - v_x \dot{\psi} . \quad (16)$$

Thereby, only the standard sensor signals of the lateral acceleration  $a_y$  and of the yaw rate  $\dot{\psi}$  are utilized. A simple proportional-integral (PI) controller (*Block 6*)

$$M_z^{\text{fb}} = k_p(\dot{v}_y^r - \dot{v}_y) + k_i \int_0^t (\dot{v}_y^r - \dot{v}_y) dt \quad (17)$$

is used as a feedback controller where  $k_p$  and  $k_i$  serve as free tuning parameters.

The required yaw torque  $M_z^c = M_z^{\text{ff}} + M_z^{\text{fb}}$ , consisting of the feedforward part  $M_z^{\text{ff}}$  and the feedback part  $M_z^{\text{fb}}$ , constitutes the output interface of the VDC system. This torque is realized by means of a subordinate control system and corresponding actuators (*Block 3*). The maximum transmittable yaw torque is determined by the actual grip ratio  $\mu$  and is therefore depicted as a  $\mu$ -dependent saturation element in Figure 3. The description of the realization of the fictitious control input  $M_z$  by means of the wheel torques is beyond the scope of this paper. However, this interface is an industrial standard in VDC systems for passenger vehicles and can for instance be found in [1, 6]. *Block 4* refers to the test vehicle equipped with the sensors for the lateral acceleration  $a_y$ , the yaw rate  $\dot{\psi}$ , and the longitudinal velocity  $v_x$ .

## 5 Stability considerations

Clearly, the control performance and the driving stability of the vehicle in terms of [5] are evaluated by means of extensive simulations with a detailed multibody vehicle model. For analyzing the stability of the closed-loop system and for estimating an admissible range of the controller parameters  $k_p$  and  $k_i$  in (17), let us consider the nonlinear single-track model according to equations (2) and (3), linearized around an arbitrary equilibrium point  $M_z = M_{z0}$ ,  $\delta_f = \delta_{f0}$ ,  $v_y = v_{y0}$  and  $\dot{\psi} = \dot{\psi}_0$ :

$$\frac{d}{dt} \begin{bmatrix} \Delta v_y \\ \Delta \dot{\psi} \end{bmatrix} = A \begin{bmatrix} \Delta v_y \\ \Delta \dot{\psi} \end{bmatrix} + B_\delta \Delta \delta_f + B_M \Delta M_z . \quad (18)$$



Thereby, the symbol  $\Delta$  describes the deviation of the corresponding quantity from the equilibrium point. Furthermore, the dynamics matrix  $A$  and the vector  $B_M$  read as

$$A = \begin{bmatrix} -\frac{1}{m}(\chi_f + \chi_r) & \frac{1}{m}(\chi_r l_r - \chi_f l_f) - v_x \\ \frac{1}{I_z}(\chi_r l_r - \chi_f l_f) & -\frac{1}{I_z}(\chi_f l_f^2 + \chi_r l_r^2) \end{bmatrix}, \quad B_M = \begin{bmatrix} 0 \\ \frac{1}{I_z} \end{bmatrix}, \quad (19)$$

with the abbreviations

$$\chi_f = \left( \frac{\partial}{\partial \alpha_f} F_f \right) (\alpha_{f0}) \frac{v_x \cos(\delta_{f0})}{v_x^2 + (v_{y0} + \dot{\psi}_0 l_f)^2} \quad \text{and} \quad \chi_r = \left( \frac{\partial}{\partial \alpha_r} F_r \right) (\alpha_{r0}) \frac{v_x}{v_x^2 + (v_{y0} - \dot{\psi}_0 l_r)^2}, \quad (20)$$

where  $\alpha_{f0}$  and  $\alpha_{r0}$  denote the side-slip angles of the front and rear axles due to (2) calculated for the equilibrium point under consideration. Note that matrix  $B_\delta$  from (18) will not be explicitly stated here since it has no influence on the stability of the closed-loop system. The feedback law due to equation (17) applied to the linearized system (18) for  $\dot{v}_y^r = 0$  takes the form

$$\Delta M_z = -k_p \Delta \dot{v}_y - k_i \Delta v_y = \underbrace{\left[ \frac{k_p}{I_z m}(\chi_f + \chi_r) - \frac{k_i}{I_z}, -\frac{k_p}{I_z} \left( \frac{1}{m}(\chi_r l_r - \chi_f l_f) - v_x \right) \right]}_K \begin{bmatrix} \Delta v_y \\ \Delta \dot{\psi} \end{bmatrix}, \quad (21)$$

and thus the dynamics matrix  $A_c = A + B_M K$  of the closed-loop system results in

$$A_c = \begin{bmatrix} -\frac{1}{m}(\chi_f + \chi_r) & \frac{1}{m}(\chi_r l_r - \chi_f l_f) - v_x \\ \frac{1}{I_z}(\chi_r l_r - \chi_f l_f) + \frac{k_p}{I_z m}(\chi_f + \chi_r) - \frac{k_i}{I_z} & -\frac{1}{I_z}(\chi_f l_f^2 + \chi_r l_r^2) - \frac{k_p}{I_z} \left( \frac{1}{m}(\chi_r l_r - \chi_f l_f) - v_x \right) \end{bmatrix}. \quad (22)$$

It can be easily verified by means of the Routh–Hurwitz stability criterion that  $A_c$  is a Hurwitz matrix iff the inequality conditions

$$k_p < \frac{m(\chi_f l_f^2 + \chi_r l_r^2) + I_z(\chi_f + \chi_r)}{m v_x - (\chi_r l_r - \chi_f l_f)} \quad \text{and} \quad k_i < \frac{v_x m(\chi_r l_r - \chi_f l_f) + \chi_f \chi_r (l_r + l_f)^2}{m v_x - (\chi_r l_r - \chi_f l_f)} \quad (23)$$

hold for the controller parameters  $k_p$  and  $k_i$ , with  $\chi_f$  and  $\chi_r$  due to (20) provided that  $m v_x - (\chi_r l_r - \chi_f l_f) > 0$ . In fact the actual values of the controller parameters  $k_p$  and  $k_i$  are determined by tuning the performance of the closed-loop system in simulation studies and experimental tests.

However, one should bear in mind that although we can guarantee exponential stability around every possible equilibrium point, this analysis does not rigorously prove the stability of the nonlinear closed-loop system comprising the nonlinear vehicle model, the feedforward, and the feedback controller. Clearly, the analysis made so far for the linearized model only gives a necessary condition for stability and the inequality conditions (23) can be considered to provide useful estimates for the bounds of the controller gains. The reader should note that most of the stability conditions being given for vehicle dynamics control in the literature are based on linearization arguments and thus are only necessary but not sufficient for the nonlinear vehicle model. The reason for this is that a rigorous stability proof of the overall nonlinear closed-loop system is indeed a very difficult task. For the two degrees-of-freedom control structure, as proposed in this paper, it is well known that in the case when the model for controller design is ideally matching the real system and has consistent initial conditions, then the feedforward controller  $M_z^{\text{ff}}$  due to (15) inserted into the system equations (2), (3) for the yaw torque  $M_z$  yields the system in Brunovsky canonical form [27]. In order to cope with model uncertainties and disturbances the feedback part due to (17) is included. The resulting error dynamics is a nonlinear time-varying system and its stability can be investigated by utilizing the Theorem of Kelemen, see, e.g., [28–30]. This theorem provides a sufficient condition and thus often turns out to be rather restrictive. The application of this theorem to a number of selected points of practical interest for the closed-loop system under consideration proves a

stable behavior. Nevertheless, the investigation of all possible operating points is in our case numerically extremely expensive and thus was omitted.

## 6 Simulation studies

In this section the performance of the presented control approach is tested by means of simulations with a detailed multibody vehicle model implemented in SIMPACK [31]. The considered vehicle model has 49 states and 35 constraints, and accordingly possesses 14 degrees-of-freedom. As a tire model Pacejka's Magic Formula [20,32] is chosen. The testing maneuver is a single lane change performed at the velocity of 25 m/s (90 km/h). The amplitude of the steering wheel angle is chosen to bring the vehicle to its physical limits, i.e. lateral accelerations of about 10 m/s<sup>2</sup>.

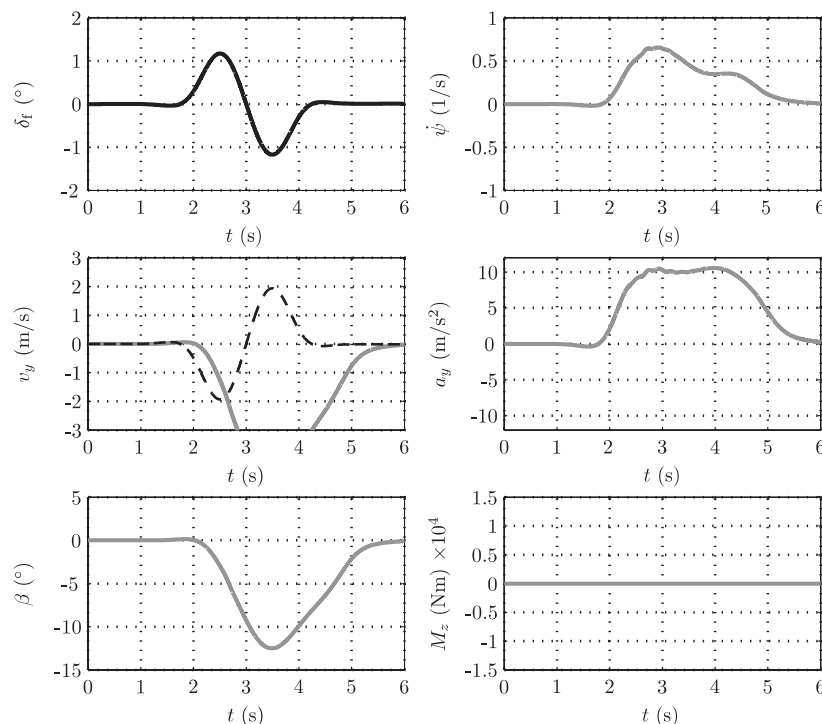


Figure 4. Simulation results of the uncontrolled detailed vehicle model, black solid line — steer angle  $\delta_f$ , dashed black line — reference trajectory  $v_y^r$ , grey solid lines — actual values.

Figure 4 shows the test maneuver performed without the control system. The black solid line refers to the steer angle  $\delta_f$ , the dashed black line to the reference trajectory  $v_y^r$  and the grey solid lines to the actual trajectories of the vehicle model, respectively. At 2.5 s the steer angle  $\delta_f$  starts to decrease but the side-slip angle  $\beta$  is still increasing for the next second. At 3 s the steer angle  $\delta_f$  even changes its sign but the side-slip angle  $\beta$ , the yaw rate  $\dot{\psi}$ , and the lateral acceleration  $a_y$  maintain the same sign until the end of the maneuver. Obviously the vehicle does not follow the steering input of the driver which corresponds to an unstable vehicle behavior.

The proposed control system (cf. Figure 3) was implemented with a sampling time of 1 ms and has shown a robust behavior. For the sake of clarity we present in Figure 5 and Figure 6 simulation results without sensor noise. During the simulations the stabilizing yaw torque  $M_z$  (shown with the solid grey line) is directly applied to the vehicle, i.e. the actuators are not explicitly considered. The feedforward part  $M_z^{\text{ff}}$  of the yaw torque is shown with the dashed black line. There is only a small corrective action of the feedback controller to compensate model inaccuracies of the simplified inverse system. The lateral velocity  $v_y$  tracks the corresponding reference trajectory  $v_y^r$  well and the side-slip angle  $\beta$  stays within  $\pm 5^\circ$ . Please note that the side-slip angle  $\beta$ , the lateral velocity  $v_y$ , and the lateral acceleration  $a_y$  are crossing zero

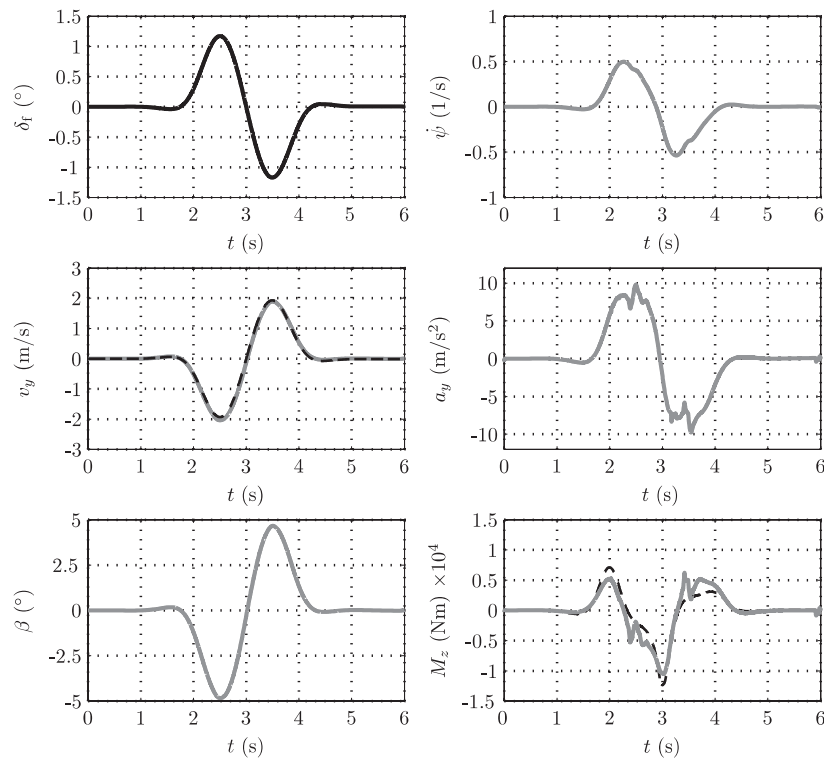


Figure 5. Simulation results of the proposed control approach with the detailed vehicle model, black solid line — steer angle  $\delta_r$ , dashed black line — reference trajectory  $v_y^r$  and feedforward yaw torque  $M_z^{\text{ff}}$  correspondingly, grey solid lines — actual values.

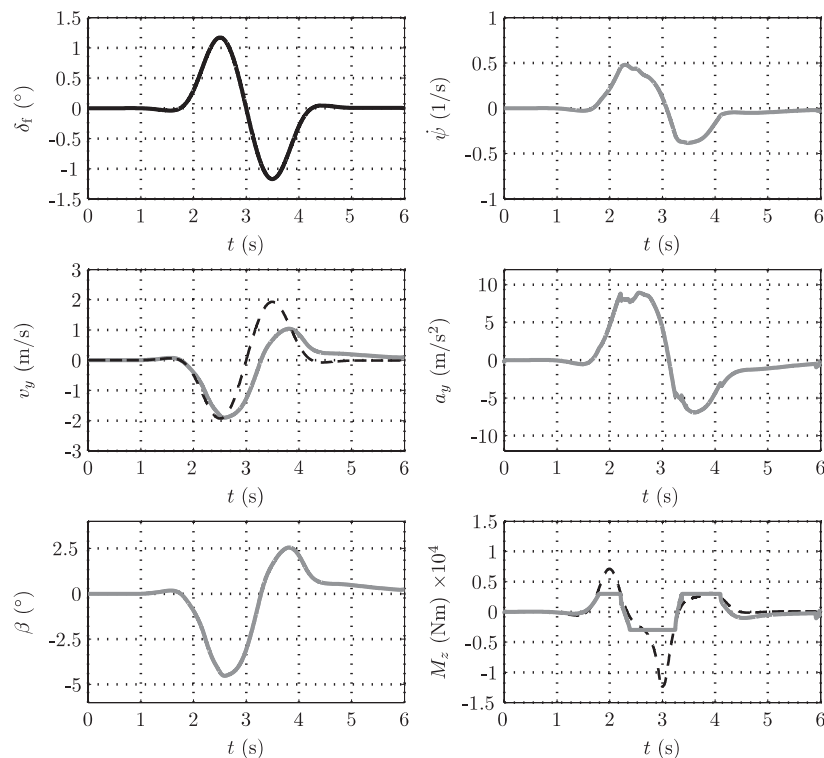


Figure 6. Simulation results of the proposed control approach with the detailed vehicle model and incorporated physical limitation of the yaw torque  $M_z$ , black solid line — steer angle  $\delta_r$ , dashed black line — reference trajectory  $v_y^r$  and feedforward yaw torque  $M_z^{\text{ff}}$  correspondingly, grey solid lines — actual values.

at the same time as the steer angle  $\delta_f$ . The yaw rate  $\dot{\psi}$  reaches the zero point *even earlier*. This shows that the usage of the inverse system allows us to achieve the maximum possible agility of the vehicle. The spikes in the lateral acceleration  $a_y$  result from suspension impacts and do not occur during less critical driving maneuvers.

Figure 6 shows the simulation results for the case where the physical limits for the stabilizing yaw torque  $M_z$  are taken into account. There is some maximum force that can be transmitted from the road to the vehicle according to the grip conditions. In this case the lateral velocity  $v_y$  can no longer follow the reference trajectory. Nevertheless, the control system tries to do its best to stabilize the vehicle. As shown in Figure 6 also in this case the side-slip angle is never exceeding  $5^\circ$ . Hence, with the proposed control concept a good trade-off between agility and stability is obtained.

Additionally, the robustness of the controller as to parameter variations and disturbances was tested by means of numerous simulations. It turned out that the proposed control concept shows a good robustness property.

## 7 Conclusion

In this contribution a systematic mathematical modeling and nonlinear control design for a vehicle dynamics control system (VDC) was presented. In order to provide a modular concept the yaw torque  $M_z$  was chosen as the control input to the system. The nonlinear control design relies on a flatness based feedforward controller and a simple linear feedback law of the time derivative of the flat output, which in our case is given by the lateral vehicle velocity  $v_y$ . Advantageously this allows us to realize a body side-slip angle control of the vehicle by means of the standard VDC system hardware. Simulation results have shown excellent control performance and a favorable trade-off between agility and stability of the vehicle. Further research deals with the consideration of the actuator dynamics and an extension of the control concept by parameter estimation algorithms.

## References

- [1] van Zanten, A., Erhardt, R., and Pfaff, G., FDR — Die Fahrdynamikregelung von Bosch, *ATZ Automobiltechnische Zeitschrift*, vol. 96, no. 11, pp. 674–689, 1994.
- [2] Donges, E., and Naab, K., Regelsysteme zur Fahrzeugführung und -stabilisierung in der Automobiltechnik, *at Automatisierungstechnik*, vol. 44, no. 5, pp. 226–236, 1996.
- [3] Lie, A., Tingvall, C., Krafft, M., and Kullgren, A., The Effectiveness of ESC (Electronic Stability Control) in Reducing Real Life Crashes and Injuries, *Proc. of the 19th Int. Techn. Conf. on the Enhanced Safety of Vehicles (ESV)*, no. 05-0135, June 2005, Washington D.C., USA.
- [4] Papelis, Y.E., Brown, T., Watson, G., Holtz, D., and Pan, W., Study of ESC Assisted Driver Performance Using a Driving Simulator, no. N04-003-PR, National Advanced Driving Simulator, The University of Iowa, USA
- [5] Inagaki, S., Kshiro, I., and Yamamoto, M., Analysis on Vehicle Stability in Critical Cornering Using Phase-Plane Method, *Proc. of the Int. Symp. on Advanced Vehicle Control (AVEC)*, no. 9438411, pp. 287–292, October 1994, Tsukuba, Japan.
- [6] Shibahata, Y., Shimada, K., and Tomari, T., Improvement of Vehicle Maneuverability by Direct Yaw Moment Control, *Vehicle System Dynamics*, vol. 22, pp. 465–482, 1993.
- [7] Drakunov, S.V., Ashrafi, B., and Rosigioni, A., Yaw Control Algorithm via Sliding Mode Control, *Proc. of the American Control Conference (ACC)*, pp. 580–583, June 2003, Chicago, Illinois, USA.
- [8] Ackermann, J., Safe and Comfortable Travel by Robust Control, In: Isidori, A., (ed.) *Trends in Control*, Springer-Verlag, London, 1995.
- [9] Tøndel, P., and Johansen, T.A., Lateral Vehicle Stabilization Using Constrained Nonlinear Control, *Proc. of European Control Conference*, 2003, Cambridge, UK.
- [10] Orend, R., Steuerung der ebenen Fahrzeugbewegung mit optimaler Nutzung der Kraftschlusspotentiale aller vier Reifen, *at Automatisierungstechnik*, vol. 53, no. 1, pp. 20–27, 2005.
- [11] Chou, H., and D’Andréa-Novel, B., Global vehicle control using differential braking torques and active suspension forces, *Vehicle System Dynamics*, vol. 43, no. 4, pp. 465–482, 2005.
- [12] Rittenschober, T., Fischer, P., Schlacher, K., and Fuchshummer, S., Fahrdynamikregelung mit differentialgeometrischen Methoden der Regelungstechnik, In *Tagungsband Internationales Forum Mechatronik*, Bayerisches Kompetenznetzwerk für Mechatronik, pp. 31–50, June 2005, Augsburg, Germany.
- [13] Burgio, G., and Zegelaar, P., Integrated vehicle control using steering and brakes, *Int. J. of Control*, vol. 79, no. 5, pp. 534–541, May 2006.
- [14] Fuchshummer, S., Schlacher, K., and Rittenschober, T., Ein Beitrag zur nichtlinearen Fahrdynamikregelung: die differentielle Flachheit des Einspurmodells, *e & i*, vol. 122, no. 9, pp. 319–324, 2005.
- [15] Fuchshummer, S., Schlacher, K., and Rittenschober, T., Nonlinear Vehicle Dynamics Control – A Flatness Based Approach, *Proc. of the 44th IEEE CDC-ECC*, pp. 6492–6497, December 2005, Séville, Spain
- [16] Horowitz, I.M., *Synthesis of Feedback Systems*, Academic Press, 1963, New York, 1963.

- [17] Hagenmeyer, V., and Zeitz, M., Flachheitsbasierter Entwurf von linearen und nichtlinearen Vorsteuerungen, *at Automatisierungstechnik*, vol. 52, no. 1, pp. 3–12, 2004.
- [18] Riekert, P., and Schnuck, T.E., Zur Fahrmechanik des gummibereiteten Kraftfahrzeugs, *Ingenieur Archiv*, vol. XI, pp.210-224, 1940.
- [19] Mitschke, M., and Wallentowitz, H., *Dynamik der Kraftfahrzeuge*, 4th edition, Springer, Berlin Heidelberg, 2004.
- [20] Pacejka, H.B., *Tyre and Vehicle Dynamics*, Elsevier Butterworth-Heinemann, Oxford, 2002.
- [21] Hackenberg, U., and Heißling, B., Die fahrdynamischen Leistungen des Fahrer–Fahrzeug–Systems im Straßenverkehr, *ATZ Automobiltechnische Zeitschrift*, vol. 84, no. 7/8, pp. 341–345, 1982.
- [22] Fliess, M., Lévine, J., Martin, P., and Rouchon, P., On differentially flat nonlinear systems, In Fiess, M., (ed.) *Nonlinear Control Systems Design*, pp. 408–412, Pergamon Press, 1992.
- [23] Fliess, M., Lévine, J., Martin, P., and Rouchon, P., A Lie–Bäcklund Approach to Equivalence and Flatness of Nonlinear Systems, *IEEE Transactions on Automatic Control*, vol. 44, no. 5, pp. 922–937, 1999.
- [24] Rathinam, M., and Murray, R.M., Configuration Flatness of Lagrangian Systems Underactuated by One Control, *SIAM Journal on Control and Optimization*, vol. 36, no. 1, pp. 164–179, 1998.
- [25] Rudolph, J., *Beiträge zur flachheitsbasierten Folgeregelung linearer und nichtlinearer Systeme endlicher und unendlicher Dimension*, Shaker Verlag, Aachen, 2003.
- [26] Reger, J., Sira–Ramírez, H., and Fliess, M., On non–asymptotic observation of nonlinear systems, *Proc. of the 44th IEEE CDC-ECC*, pp. 4219–4224, December 2005, Séville, Spain.
- [27] Isidori, A., *Nonlinear Control Systems*, 3rd edition, Springer–Verlag, London, 2001.
- [28] Hagenmeyer, V., *Robust Nonlinear Tracking Control based on Differential Flatness*, VDI–Verlag, Düsseldorf, 2003.
- [29] Kelemen, M., A stability property, *IEEE Transactions on Automatic Control*, vol. 31, pp. 766–768, 1986.
- [30] Lawrence, A.L., and Rugh, W.J., On a stability theorem for nonlinear systems with slowly varying inputs, *IEEE Transactions on Automatic Control*, vol. 35, pp. 860–864, 1990.
- [31] SIMPACK, available online <http://www.simpack.com>.
- [32] Bakker, E., Nyborg, L., and Pacejka, H.B., Tyre Modelling for Use in Vehicle Dynamics Studies, *SAE Technical Paper Series*, no. 870421, 1987.